Temperature-based Instanton Analysis: Identifying Vulnerability in Transmission Networks

Jonas Kersulis, Ian Hiskens
Elec. Eng. and Computer Science
University of Michigan
Ann Arbor, MI, United States

Michael Chertkov, Scott Backhaus
Center for Nonlinear Studies
Los Alamos National Laboratory
Los Alamos, NM, United States

Daniel Bienstock
Ind. Eng. and Operations Research
Columbia University
New York, NY, United States

***Abstract*—A time-coupled instanton method for characterizing transmission network vulnerability to wind generation fluctuation is presented. To extend prior instanton work to multiple-time-step analysis, line constraints are specified in terms of temperature rather than current. An optimization formulation has been developed that determines the minimum deviation in wind power from the forecast such that line temperature is driven to its limit. Results are shown for an IEEE RTS-96 system with several wind farms.**

***Index Terms*—Forecast uncertainty, Optimization, Transmission operations, Wind energy**

I. Introduction

The prevalence of renewables in modern transmission networks has researchers and system operators asking: What happens when the wind changes, and could fluctuations harm the grid? The instanton problem provides an answer, and this paper extends instanton analysis to the temporal setting. Though small deviations from wind forecasts are typically harmless, it is possible for certain wind generation patterns to drive the system to an infeasible operating point. Out of all troublesome wind generation patterns, the one that deviates least from the forecast is called the instanton. Instanton analysis uses optimization to find the set of troublesome wind patterns (each of which causes a particular line to encounter its flow limit). By ranking these wind patterns according to distance from forecast, we can characterize the system's vulnerability to forecast inaccuracy and enhance system operator awareness.

Previous work has solved several variants of the instanton problem. In 2012 [1] used the physically accurate AC power flow equations and found instanton candidates with an iterative scheme. Other papers, including [2] and [3], have used the DC power flow approximation to turn instanton analysis into a convex problem with an analytic solution. Current instanton research is exploring the trade-off between problem complexity and solution accuracy, with the goal of developing the most accurate model that remains convex (and therefore guarantees a solution). To the authors' knowledge, all instanton work to date has focused on instantaneous vulnerability. In other words, prior work has assumed fixed demand and generator dispatch, and has used power or current limits as constraints. Thus, the troublesome wind patterns uncovered by instanton analysis may be fleeting.

It is safe to temporarily operate a line above its current limit. Transmission system operators know this and periodically allow lines to operate above their limits to promote smooth operation under heavy load (see the introduction of [4] for a history of dynamic line rating starting in the 1970s). It takes time for a line to accumulate enough heat to cause it to sag to an unacceptable level (as defined by statute and nearby tree limbs). As long as the line is allowed to cool before reaching this point, no harm will be done. If an operator is comfortable with temporarily overloaded lines, information from today's instanton analysis may be too conservative to aid in decision making.

In this paper we bring instanton analysis into the temporal setting. We consider multiple time steps and replace line current limits with heat constraints. A line's temperature is a function of heat input (primarily Ohmic losses and heat from the sun) and dissipation (convection and radiation, which depend on ambient conditions), and is represented as a differential equation (see Section 3.4 of [5] for a standard set of equations governing line temperature dynamics). Ohmic loss heating is related to power flow analysis via angle difference variables. By modeling line temperature over a significant time horizon, the new method discovers multiple-time-step wind patterns that are both likely to occur and sure to induce excessive sag for at least one line in the network.

The remainder of the paper describes the temporal instanton problem (Section II), translates it into an optimization problem (Section III), presents a solution method (Section IV), and illustrates temporal instanton analysis using a modified RTS-96 network (Section V).

II. Problem formulation

Section II-A describes an approximate line loss formulation that forms the basis of a dynamical model developed in Section II-B. Finally, Section II-C incorporates line temperature dynamics into a complete mathematical model.

A. Line losses

Starting with the AC line loss expression, [6] derived the following approximate relationship between line losses and

The authors acknowledge the support of the Los Alamos National Laboratory Grid Science Program, subcontract 270958.

TABLE I
LINE HEATING PARAMETERS

Parameter	Units	Description
T_s	s	Sample time
mC_p	$J/(m \cdot C)$	Per-unit-length heat capacity of the conductor
η_c	$W/(m \cdot C)$	Conductive heat loss rate coefficient
η_r	$W/(m \cdot C)$	Radiative heat loss rate coefficient
T^{lim}	C	Line temperature at steady-state current limit.
$\Delta q_{s,ij}$	W/m	Solar heat input into conductor
ΔT_{amb}	C	Change in ambient temperature

voltage angle differences for line (i, j):

$$f_{ij}^{\text{loss}} \approx r_{ij} \left(\frac{\theta_{ij}}{x_{ij}} \right)^2 \tag{1}$$

In this expression, f_{ij}^{loss} is the approximate active power loss on the line, and θ_{ij} is the difference between angles θ_i and θ_k. r_{ij} and x_{ij} are the resistance and reactance of the line, respectively. Equation (1) is predicated on three assumptions: voltage magnitudes are all 1 pu, cosine may be approximated by its second-order Taylor expansion, and $x_{ij} \geq 4r_{ij}$. Thus, (1) uses DC power flow assumptions to approximate line losses, but remains nonlinear.

B. Line temperature dynamics

According to analysis done in [6] (which is based on [5]), changes in line temperature may be calculated using the following Euler integration:

$$\Delta T_{ij}[t+1] = \tau_{ij} \Delta T_{ij}[t] + \rho_{ij} \Delta f_{ij}^{\text{loss}}[t] + \delta_{ij} \Delta d_{ij}[t] \ , \tag{2}$$

where the initial condition is $\Delta T_{ij}[0] = 0$. Constants τ_{ij} and $\bar{\gamma}_c$ are defined as

$$\tau_{ij} = 1 - \frac{T_s \bar{\gamma}_c}{mC_p}, \qquad \bar{\gamma}_c = \eta_c + 4\eta_r (T^{\text{lim}} + 273)^3 \ , \tag{3}$$

and $\rho_{ij} = T_s / mC_p$. Finally, $\Delta d_{ij} = \text{col}(\Delta q_{s,ij}, \Delta T_{\text{amb}})$, and δ_{ij} represents exogenous inputs and is equal to $[\rho_{ij} \ \gamma_{ij}]$, where

$$\gamma_{ij} = \frac{T_s \bar{\gamma}_a}{mC_p}, \qquad \bar{\gamma}_a = \eta_c + 4\eta_r (T^*_{\text{amb}} + 273)^3 \ . \tag{4}$$

Integration sample time is constrained by numerical stability requirements, which necessitate $\tau_{ij} \in (-1, 1)$:

$$T_s < \min_{ij} \left\{ \frac{2mC_{p,ij}}{\bar{\gamma}_{c,ij}} \right\} \tag{5}$$

The collection of line temperature parameters in (2)-(5) is summarized in Table I.

If line parameters and ambient conditions are considered fixed with respect to power flow, (2) is a recursive relationship between angle difference variables $\theta_{ij}[t+1]$ and $\theta_{ij}[t]$. Repeated substitution and use of (1) yields an expression for the change in line temperature at a final time in terms of angle differences at all other time steps. If there are T total time steps, this relationship may be expressed as follows:

$$\Delta T_{ij}[T] = \frac{\rho_{ij} r_{ij}}{x_{ij}^2} \sum_{t=1}^{T} \tau_{ij}^{t-1} \theta_{ij}^2 [T+1-t] \ + \\ + \delta_{ij} \sum_{t=1}^{T} \tau_{ij}^{t-1} \Delta d_{ij}[T+1-t] \tag{6}$$

The first term in (6) varies with angle differences. The second term, which is based on external conditions, is constant with respect to all power flow variables. Switching the order of summation and moving constants to the left side yields

$$\Delta T_{ij}[T] - \delta_{ij} \sum_{t=1}^{T} \tau_{ij}^{T-t} \Delta d_{ij}[t] = \\ = \frac{\rho_{ij} r_{ij}}{x_{ij}^2} \sum_{t=1}^{T} \tau_{ij}^{T-t} \theta_{ij}^2 [t] \ . \tag{7}$$

This form suggests a quadratic matrix-vector expression, which we obtain by first defining an angle difference vector, a constant vector, and a coefficient matrix:

$$\boldsymbol{\theta}_{ij} := \begin{bmatrix} \theta_{ij}[1] & \theta_{ij}[2] & \cdots & \theta_{ij}[T] \end{bmatrix}^\top \tag{8a}$$

$$\boldsymbol{\Delta d}_{ij} := \begin{bmatrix} \Delta d_{ij}[1] & \Delta d_{ij}[2] & \ldots & \Delta d_{ij}[T] \end{bmatrix}^\top \tag{8b}$$

$$\boldsymbol{\tau}_{ij} := \text{diag} \left(\begin{bmatrix} \tau_{ij}^{T-1} & \tau_{ij}^{T-2} & \cdots & 1 \end{bmatrix} \right) \tag{8c}$$

In terms of these newly-defined symbols (whose dependence on T is hidden for conciseness), (7) becomes

$$\Delta T_{ij}[T] - \delta_{ij} \boldsymbol{\Delta d}_{ij}^\top \boldsymbol{\tau}_{ij} \mathbf{1} = \frac{\rho_{ij} r_{ij}}{x_{ij}^2} \boldsymbol{\theta}_{ij}^\top \boldsymbol{\tau}_{ij} \boldsymbol{\theta}_{ij} \ . \tag{9}$$

The left side of (9) is constant with respect to power flow, and the right side is a weighted, scaled two-norm of the vector of angle difference variables $\boldsymbol{\theta}_{ij}$.

The approximate line temperature dynamics developed here will be used in Section III to keep track of line temperature over an optimization horizon.

C. Instanton formulation

The preceding discussion used an approximate line loss expression to relate line temperature to angle variables according to (9). Here we describe the remaining parts of the temporal instanton model.

The following equations describe an optimization problem that minimizes deviation from the wind forecast while heating

a certain line to an unacceptable temperature:

$$\min \sum_{t=1}^{T} dev_t^\top Q_{dev} dev_t \tag{10a}$$

subject to:

$$\sum_j Y_{ij}\theta_{ij,t} = G_{i,t} + R_{i,t} + dev_{i,t} - D_{i,t} \qquad \forall i \in 1...N,\ t \in 1...T \tag{10b}$$

$$G_t = G_{0,t} + k\alpha_t \quad \forall t \in 1 \dots T \tag{10c}$$

$$\theta_{ref,t} = 0 \quad \forall t \in 1 \dots T \tag{10d}$$

$$\Delta T_{ij}[T] = \Delta T_{ij}^{\lim} \quad \text{for some } (i,j) \in \mathcal{G} \tag{10e}$$

Where:

- $dev_{i,t}$ is the difference between actual output and forecast output at wind farm i and time t. Thus, dev_t is the vector of wind forecast deviations at time t.
- Q_{dev} may be set to the identity matrix or used to encode correlation between wind sites.
- $R_{i,t}$ is renewable generation forecast at bus i and time t.
- Y_{ij} is the (i,j)-th element of the admittance matrix, which assumes zero resistance.
- $\theta_{ij,t}$ is the difference between the bus i phase angle and the bus k phase angle at time t.
- $G_{i,t}$ is conventional active power generation at node i and time t, and G_t is a vector including all nodes.
- $D_{i,t}$ is active power demand at bus i and time t.
- N is the number of buses (nodes).
- $G_{0,t}$ is scheduled conventional active power generation (without droop response).
- k is the vector of participation factors for conventional generators, with $\sum_i k_i = 1$. (The case where $k_i = 1$ corresponds to generator i taking all slack.)
- α_t is the mismatch at time t, defined as
$$\alpha_t := \sum D_t - \sum \rho_t - \sum G_{0,t}\ .$$
- ΔT_{ij}^{lim} is the change in temperature that will push line (i,j) to its thermal limit.
- θ_{ref} is the phase angle of the reference bus (fixed at zero).
- $\mathcal{G}$ is the set of edges (lines).

Equation (10a) expresses the desire to find wind patterns that remain close to the wind forecast. The first constraint equation (10b) enforces DC power balance. The next constraint (10c) models conventional active power generation as a sum of scheduled generation and droop response (where generators share the task of compensating for mismatch between total generation and total load). The system angle reference is established by (10d). Last is (10e), which constrains the temperature of a particular line to be equal to its limit at the final time t_{end}. Using (9) we can express (10e) as

$$\Delta T_{ij}^{lim} - \delta_{ij}\boldsymbol{\Delta d}_{ij}^\top \boldsymbol{\tau}_{ij}\mathbf{1} = \frac{\rho_{ij} r_{ij}}{x_{ij}^2}\boldsymbol{\theta}_{ij}^\top \boldsymbol{\tau}_{ij}\boldsymbol{\theta}_{ij}\ . \tag{11}$$

Thus, (10) has a quadratic objective function, a set of linear constraints, and a single quadratic constraint. By solving (10) for each line in the network, we obtain a set of instanton candidate wind patterns, each of which will heat a particular line to its thermal limit. Of these candidates, the one that deviates least from the wind forecast (across all time steps) is the instanton wind pattern.

The form of (10) suggests a QCQP optimization formulation. The next section describes such a QCQP in full detail.

III. Conversion to optimization problem

Previous instanton work relied on convex optimization to quickly find instanton wind patterns. Heat-constrained temporal instanton analysis introduces significant complication: it cannot be formulated as anything simpler than a quadratically-constrained quadratic program (QCQP). QCQPs are NP-hard in general; reasonable solutions may exist, but unless the quadratic constraint matrices are positive-definite there is no solution guarantee (see [7]). Because system operators require robustness, "no solution found" is an unacceptable output. With this criterion in mind, we proceed to develop an optimization model whose structure permits us to find solutions despite nonconvexity.

With all deviation, angle, and mismatch variables stacked into a single vector, (10) takes the following form:

$$\min z^\top Q_{obj} z \tag{12a}$$

$$s.t. \quad Az = b \tag{12b}$$

$$z^\top Q_\theta z = c \tag{12c}$$

The objective (12a) is equivalent to (10a), the linear equality constraints (12b) represent (10b)-(10d), and the quadratic equality constraint (12c) is equivalent to (10e). z consists of $(N+N_R+2)T$ variables, where N is the number of nodes, N_R is the number of nodes with wind farms, and T is the number of time steps. $N_R T$ of the variables represent deviations from forecast at each wind farm and time step. There are also NT variables (of which T are fixed to zero according to (10d)) and T mismatch variables α_t (one per time step). The last T variables are used to convert the quadratic constraint (10e) into a norm constraint; they are defined later on in (15).

Variables may be stacked in any order. One convenient ordering is T groups of $(N + N_R + 1)$ variables, with the T auxiliary angle difference variables at the end. At a particular time step t, the group of $(N + N_R + 1)$ variables is $[dev_t^\top \quad \theta_t^\top \quad \alpha_t]^\top$. dev_t represents deviations from forecast at the N_R wind nodes, θ_t is the column of N angle variables at time t, and α_t is the mismatch between generation and demand at time t.

The remainder of this section describes each of the four components of (12). The objective matrix Q_{obj} is described in Section III-A, linear constraint parameters A and b are considered in Section III-B, and the constraint matrix Q_θ is addressed by Section III-C.

A. Objective function and Q_{obj}

The objective function depends solely on deviation variables, so Q_{obj} is a matrix that weights only the dev variables

in z. If there are two time steps, for example, the vector of variables would be $z = \begin{bmatrix} dev_t^\top & \theta_1^\top & \alpha_1 & dev_2^\top & \theta_2^\top & \alpha_2 & \hat{\theta} \end{bmatrix}^\top$, and Q_{obj} would be

$$Q_{obj} = \begin{bmatrix} Q_{dev} & 0 & 0 & 0 & 0 & 0 \\ 0 & 0 & 0 & 0 & 0 & 0 \\ 0 & 0 & 0 & 0 & 0 & 0 \\ 0 & 0 & 0 & Q_{dev} & 0 & 0 \\ 0 & 0 & 0 & 0 & 0 & 0 \\ 0 & 0 & 0 & 0 & 0 & 0 \end{bmatrix} .$$

Note that Q_{dev} represents the correlation between wind farms (if any). In the Section IV numerical analysis, we will assume $Q_{dev} = I$, the identity matrix.

B. Linear constraints: A and b

All constraints except the temperature limit may be grouped into a single linear system $Az = b$. Setting aside the T auxiliary variables for the moment, the A matrix has a block diagonal structure where each block consists of $(N+1)$ rows and $(N_R + N)$ columns. The first N rows describe power balance and distributed slack behavior at each node. For node i and time t, we fix elements of A and b to establish

$$\sum_j Y_{ij}\theta_{j,t} = (G^0_{i,t} + k_i\alpha_t) + (\rho_{i,t} + dev_{i,t}) - D_{i,t} \ . \quad (13)$$

The first pair of terms on the right-hand side of (13) represents conventional generation with distributed slack (generator i is taking a portion k_i of the mismatch α_t). The second pair of terms is renewable generation: forecast $R_{i,t}$ plus deviation $dev_{i,t}$. The final term is demand at node i and time t. (Note that renewable generation terms are zero for nodes without wind farms.) In addition to the N rows corresponding to (13) at the N nodes, there is one additional equation associated with time t that fixes α_t:

$$\alpha_t = \sum_i \left(D_{i,t} - G^0_{i,t} - (R_{i,t} + dev_{i,t})\right) \quad (14)$$

(Note that α_t is positive when demand exceeds generation. This causes conventional generators to increase output according to (10c).)

The $(N+1)$ rows of $Az = b$ expressed in (13) and (14) pertain to a single time step t. T blocks of this form are arranged diagonally to form $(N+1)T$ rows of A and elements of b. There is one additional block of A used to define angle difference variables $\hat{\theta}_{ij,t}$ in terms of angle variables $\theta_{i,t}$ and $\theta_{j,t}$ at each time step:

$$\hat{\theta}_{ij,t} = \tau^{\frac{T-t}{2}}(\theta_{i,t} - \theta_{j,t}) \ . \quad (15)$$

The next subsection explains why these auxiliary variables $\hat{\theta}$ are helpful.

C. Quadratic constraint: Q_θ and c

Recall that (11) describes the temperature constraint on a chosen line (i, j). We can rearrange (11) into the form of (12c), with all constants on the right side:

$$\boldsymbol{\theta}_{ij}^\top \boldsymbol{\tau}_{ij} \boldsymbol{\theta}_{ij} = \frac{x_{ij}^2}{\rho_{ij} r_{ij}} \left(\Delta T_{ij}^{lim} - \delta_{ij} \boldsymbol{\Delta} \boldsymbol{d}_{ij}^\top \boldsymbol{\tau}_{ij} \mathbf{1}\right) \quad (16)$$

This makes it clear that the appropriate value of c in (12c) is

$$c = \frac{x_{ij}^2}{\rho_{ij} r_{ij}} \left(\Delta T_{ij}^{lim} - \delta_{ij} \boldsymbol{\Delta} \boldsymbol{d}_{ij}^\top \boldsymbol{\tau}_{ij} \mathbf{1}\right) \quad (17)$$

From the definition of $\hat{\theta}_{ij,t}$ in (15), we see that the left side of (16) may be expressed as $\hat{\theta}_{ij}^\top \hat{\theta}_{ij}$. Thus, if the $\hat{\theta}_{ij}$ variables are placed at the bottom of z, Q_θ must be a matrix of zeros with a T-by-T identity matrix in the lower-right corner. This ensures that $z^\top Q_\theta z = \hat{\theta}_{ij}^\top \hat{\theta}_{ij}$, as desired.

Section II described the temporal instanton problem, Section III expressed it as a QCQP, and this section defined each component. Next we present a solution method for (12).

IV. Solution

The structure of (12) is similar to that of the well-known trust region subproblem. Here we describe a four-step solution method based in part on [8]. We begin by considering the vector of variables z as three groups: $z_1 \in \mathbb{R}^{N_R T}$ contains all wind deviations, $z_2 \in \mathbb{R}^{(N+1)T}$ contains angle and mismatch variables, and $z_3 \in \mathbb{R}^T$ contains auxiliary angle difference variables involved in line temperature calculation. (This partition of z is independent of how the variables are ordered.) With this notation, the problem becomes

$$\begin{aligned} & \min \ z_1^\top \left(\text{diag}_T(Q_{dev})\right) z_1 && (18a) \\ s.t. \quad & Az = b && (18b) \\ & z_3^\top z_3 = c \ , && (18c) \end{aligned}$$

where $\text{diag}_T(Q_{dev})$ represents Q_{dev} repeated in block-diagonal fashion T times.

Several changes of variables may be used to obtain an equivalent, but much simpler, form of (18).

A. Translation

The first step is to change variables from z to $y = z - z^*$, where $z^* \in \{z : Az = b\}$. This translation transforms $Az = b$ into $Ay = 0$. To prevent the change from introducing a linear term into the quadratic constraint, we require $z_3^* = 0$. To satisfy $Az^* = b$, then, z_1^* and z_2^* must satisfy

$$A \begin{bmatrix} z_1^* \\ z_2^* \\ 0 \end{bmatrix} = b \ .$$

It is straightforward to find a min-norm z^* that satisfies this constraint by partitioning and factorizing A appropriately. After translation, the problem takes the form

$$\begin{aligned} & \min \ y_1^\top Q_z y_1 + 2 y_1^\top Q_z z_1^* && (19a) \\ s.t. \quad & Ay = 0 && (19b) \\ & y_3^\top y_3 = c && (19c) \end{aligned}$$

B. Kernel mapping

The form of (19b) suggests an intuitive explanation: any solution to (19) must lie in the nullspace (kernel) of A. If $\dim \mathcal{N}(A) = k$ is the dimension of this nullspace, we can replace y by Nx where $N \in \mathbb{R}^{n \times k}$ spans $\mathcal{N}(A)$. (Note that x no longer refers to reactance in this context.) This change of variables is akin to a rotation, but reduces the problem dimension to k. After the change of variables, the problem becomes

$$\min \; x^\top (N^\top Q_{obj} N)x + 2x^\top N^\top (Q_z z_1^*) \tag{20a}$$

$$s.t. \quad x^\top N_3^\top N_3 x = c \; . \tag{20b}$$

All feasible solutions to (20) lie in the nullspace of A, so the linear constraints are now implicit.

C. Obtaining a norm constraint

After kernel mapping, the quadratic constraint is no longer a norm constraint. We can fix this in two steps. First, perform an Eigendecomposition $N_3^\top N_3 = UDU^\top$ and let $\hat{x} = U^\top x$. The constraint is diagonal in terms of $\hat{x}$:

$$x^\top N_3^\top N_3 x = \hat{x}^\top D \hat{x} \tag{21}$$

D is diagonal and has at most T nonzero elements, so the right side of (21) may be expanded into

$$\begin{bmatrix} \hat{x}_1^\top & \hat{x}_2^\top \end{bmatrix} \begin{bmatrix} 0 & 0 \\ 0 & \hat{D} \end{bmatrix} \begin{bmatrix} \hat{x}_1 \\ \hat{x}_2 \end{bmatrix} \; . \tag{22}$$

The second step is to change variables from $\hat{x}$ to $w = [w_1 \; w_2]^\top$. The variables x, $\hat{x}$ and w are related as follows:

$$\begin{bmatrix} w_1 \\ w_2 \end{bmatrix} = \begin{bmatrix} I & 0 \\ 0 & \hat{D}^{1/2} \end{bmatrix} \begin{bmatrix} \hat{x}_1 \\ \hat{x}_2 \end{bmatrix} = K\hat{x} \tag{23}$$

$$\implies w = KU^\top x$$

(Note that $z = UK^{-1}w$ because $UU^\top = I$. Changing from z to w is equivalent to rotating by $(UK^{-1})^\top$.)

In terms of w, (20b) takes the form of a norm:

$$\hat{x}^\top D \hat{x} = \hat{x}_2 \hat{D}^{1/2} \hat{D}^{1/2} \hat{x}_2 = w_2^\top w_2 \; . \tag{24}$$

Of course, this change of variables also influences the cost function. After substitution and simplification, the full problem becomes

$$\min \; w^\top B w + w^\top b \tag{25a}$$

$$s.t. \quad w_2^\top w_2 = c \tag{25b}$$

where

$$B = K^{-1}U^\top N^\top Q_z N U K^{-1} \text{ and } b = 2K^{-1}U^\top N_1 z_1^* .$$

The manipulations in this section have restored the norm structure of the quadratic constraint. In the next section we use the KKT conditions of (25) to eliminate w_1, the unconstrained part of w. This will allow us to write the objective in terms of w_2 only.

D. Eliminating w_1

Note that w_1 is unconstrained in (25). For a fixed w_2, we can use the KKT conditions to find w_1 such that the objective is minimized. Begin by expanding the objective:

$$\begin{aligned} f(w) &= \begin{bmatrix} w_1^\top & w_2^\top \end{bmatrix} \begin{bmatrix} B_{11} & B_{12} \\ B_{12}^\top & B_{22} \end{bmatrix} \begin{bmatrix} w_1 \\ w_2 \end{bmatrix} + \begin{bmatrix} w_1^\top & w_2^\top \end{bmatrix} \begin{bmatrix} b_1 \\ b_2 \end{bmatrix} \\ &= w_1^\top B_{11} w_1 + 2w_1^\top B_{12} w_2 + w_2^\top B_{22} w_2 + w_1^\top b_1 + w_2^\top b_2 \end{aligned}$$

Next, set the partial derivative with respect to w_1 equal to zero:

$$\frac{\partial f}{\partial w_1} = 2w_1^\top B_{11} + 2w_2^\top B_{12}^\top + b_1^\top = 0$$

$$\iff w_1 = -B_{11}^{-1} \left(B_{12} w_2 - \frac{1}{2} b_1 \right) \tag{26}$$

After substitution of (26), the objective depends only on w_2:

$$f(w_2) = w_2^\top \left(B_{22} - B_{12}^\top B_{11}^{-1} B_{12} \right) w_2 + w_2^\top (b_2 - B_{12}^\top B_{11}^{-1} b_1) \; ,$$

(Note that the constant term, which plays no role in minimization, was omitted.) The full optimization problem becomes

$$\min \; w_2^\top \hat{B} w_2 + w_2^\top \hat{b} \tag{27a}$$

$$s.t. \quad w_2^\top w_2 = c \; , \tag{27b}$$

where

$$\hat{B} = B_{22} - B_{12}^\top B_{11}^{-1} B_{12} \text{ and } \hat{b} = b_2 - B_{12}^\top B_{11}^{-1} b_1 \; .$$

(27) is a QCQP in T dimensions with a single norm constraint. It is straightforward to obtain solutions to this problem, as the next subsection will show.

E. Solution via enumeration

Let v be the Lagrange multiplier associated with (27b) and write the first-order optimality condition for (27):

$$\frac{\partial \mathcal{L}(w_2, v)}{\partial w_2} = 2\hat{B} w_2 + \hat{b} - v(2w_2) = 0$$

$$\implies \hat{B} w_2 + \frac{1}{2} \hat{b} = v w_2 \tag{28}$$

Equation (28) is a linear system that yields w_2 for fixed v:

$$w_{2,i} = \frac{\hat{b}_i / 2}{v - \hat{B}_{i,i}} \tag{29}$$

In addition to satisfying (29), an optimal w_2 must satisfy the quadratic constraint. Substituting (29) into (27b) yields the "secular equation" (see [8]):

$$s(v) = \sum_i \left(\frac{\hat{b}_i / 2}{v - \hat{B}_{i,i}} \right)^2 = c \tag{30}$$

Note that $s(v)$ has one pole per unique nonzero diagonal element of $\hat{B}$. There are at most two solutions per pole, one on each side. This is best understood graphically. Figure 1 illustrates a secular equation with three poles, taken from analysis of the RTS-96 network. The horizontal axis is the value of the Lagrange multiplier v, and the vertical axis is the secular equation value $s(v)$. Solutions are intersections of $s(v)$ with the horizontal line $s(v) = c$. They are computed numerically with a simple binary search algorithm.

V. Results for RTS-96 network

We used data from [9] to demonstrate temporal instanton analysis on a wind-augmented RTS-96 network model. Consider a scenario unfolding over three time steps: first the wind forecast is 50% of some nominal value, next it is equal to the nominal value, and finally it is scaled to 150% of nominal. Throughout this wind ramping, generator dispatch and demand remain constant. Temporal instanton analysis with $c = 0.03$ and $\tau = 0.5$ indicates that the line between buses 121 and 325 is most susceptible to excessive heating under these conditions. In other words, of all dangerous wind patterns that could occur during the wind ramp, the most likely is a pattern that overheats the line between buses 121 and 325. Figure 1 illustrates the secular equation used to find this instanton pattern, and Figure 2 shows the system state at the second time step. The largest deviation in the instanton pattern is 0.73 pu, well within the range of wind forecast values (whose maximum is 1.2 pu).

There is a great deal of flexibility in the temporal instanton model that has yet to be explored. In future work we plan to include transformers, consider the effects of ambient conditions in greater detail, and test the limits of the algorithm using large networks with many time steps.

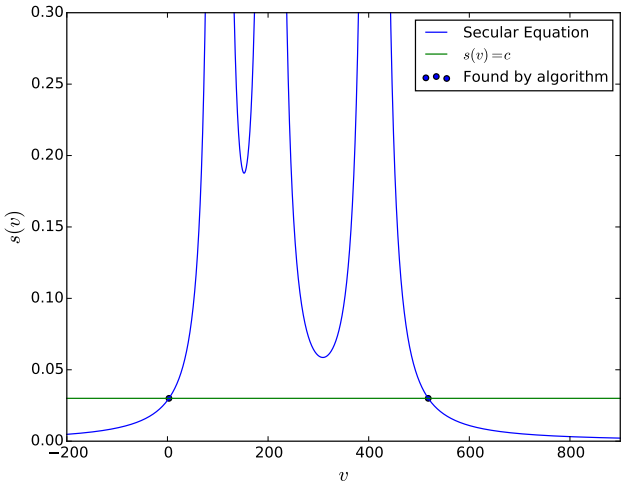

Fig. 1. Plot of secular equation for a single line in the RTS-96. Note that $s(v)$ approaches infinity at the three poles, and there could be as many as six solutions if c were large enough.

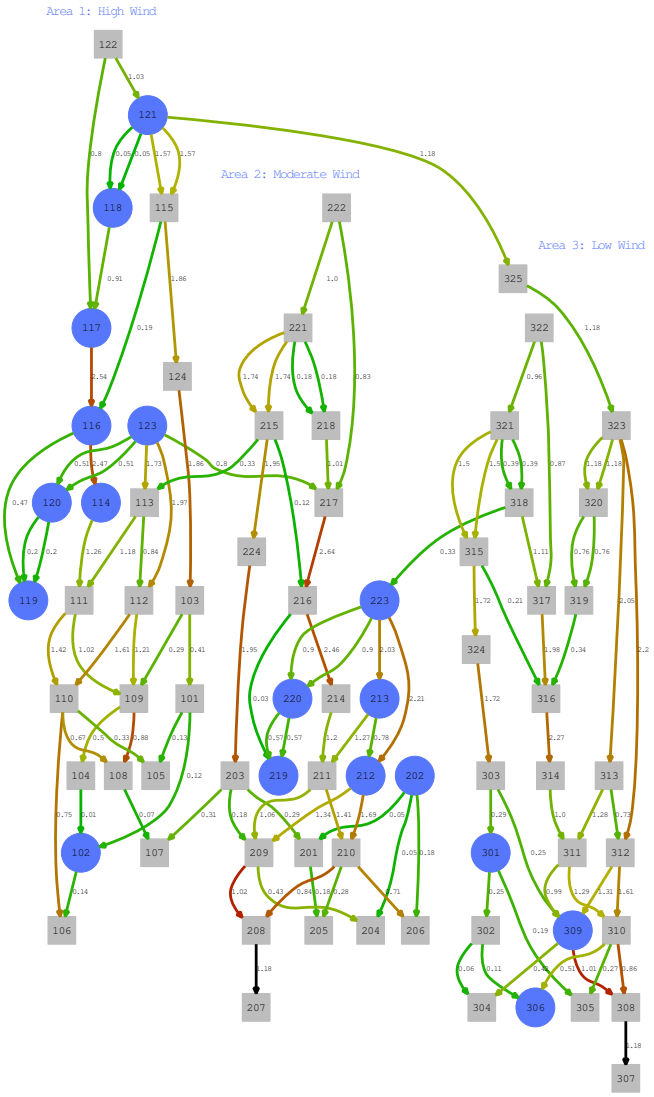

Fig. 2. Graph depiction of RTS-96 system state under instanton conditions at time step 2 of 3. The stressed line is between buses 121 and 325 (top center). Wind farms are indicated by blue, and lines are colored according to how close their flows are to static active power limits.

References

[1] S. Baghsorkhi and I. Hiskens, "Analysis tools for assessing the impact of wind power on weak grids," in *Proc. Systems Conference (SysCon), 2012 IEEE International*, 2012, pp. 1–8.

[2] M. Chertkov, F. Pan, and M. Stepanov, "Predicting failures in power grids: The case of static overloads," *IEEE Transactions on Smart Grid*, vol. 2, no. 1, pp. 162–172, Mar. 2011.

[3] M. Chertkov, M. Stepanov, F. Pan, and R. Baldick, "Exact and efficient algorithm to discover extreme stochastic events in wind generation over transmission power grids," in *Proc. 2011 50th IEEE Conference on Decision and Control and European Control Conference (CDC-ECC)*, 2011, pp. 2174–2180.

[4] H. Banakar, N. Alguacil, and F. Galiana, "Electrothermal coordination part I: theory and implementation schemes," *IEEE Transactions on Power Systems*, vol. 20, no. 2, pp. 798–805, May 2005.

[5] "IEEE standard for calculating the current-temperature of bare overhead conductors," *IEEE Std 738-2006 (Revision of IEEE Std 738-1993)*, pp. c1–59, Jan. 2007.

[6] M. Almassalkhi and I. Hiskens, "Model-predictive cascade mitigation in electric power systems with storage and renewables – part I: Theory and implementation," *IEEE Transactions on Power Systems*, vol. PP, no. 99, pp. 1–11, 2014.

[7] O. Mehanna, K. Huang, B. Gopalakrishnan, A. Konar, and N. Sidiropoulos, "Feasible point pursuit and successive approximation of non-convex QCQPs," *IEEE Signal Processing Letters*, vol. PP, no. 99, pp. 1–1, 2014.

[8] D. Bienstock and A. Michalka, "Polynomial Solvability of Variants of the Trust-region Subproblem," in *Proceedings of the Twenty-Fifth Annual ACM-SIAM Symposium on Discrete Algorithms*, ser. SODA '14. Portland, Oregon: SIAM, 2014, pp. 380–390. [Online]. Available: http://dl.acm.org/citation.cfm?id=2634074.2634102

[9] H. Pandzic, Y. Dvorkin, T. Qiu, Y. Wang, and D. Kirschen. Unit Commitment under Uncertainty - GAMS Models, Library of the Renewable Energy Analysis Lab (REAL), University of Washington, Seattle, USA. [Online]. Available: http://www.ee.washington.edu/research/real/gams_code.html